Zeitschrift: IABSE reports of the working commissions = Rapports des commissions de travail AIPC = IVBH Berichte der Arbeitskommissionen

Band: 11 (1971)

Artikel: Ultimate load and failure mechanism of thin webs in shear

Autor: Škaloud, Miroslav

DOI: https://doi.org/10.5169/seals-12056

Nutzungsbedingungen

Die ETH-Bibliothek ist die Anbieterin der digitalisierten Zeitschriften auf E-Periodica. Sie besitzt keine Urheberrechte an den Zeitschriften und ist nicht verantwortlich für deren Inhalte. Die Rechte liegen in der Regel bei den Herausgebern beziehungsweise den externen Rechteinhabern. Das Veröffentlichen von Bildern in Print- und Online-Publikationen sowie auf Social Media-Kanälen oder Webseiten ist nur mit vorheriger Genehmigung der Rechteinhaber erlaubt. Mehr erfahren

Conditions d'utilisation

L'ETH Library est le fournisseur des revues numérisées. Elle ne détient aucun droit d'auteur sur les revues et n'est pas responsable de leur contenu. En règle générale, les droits sont détenus par les éditeurs ou les détenteurs de droits externes. La reproduction d'images dans des publications imprimées ou en ligne ainsi que sur des canaux de médias sociaux ou des sites web n'est autorisée qu'avec l'accord préalable des détenteurs des droits. En savoir plus

Terms of use

The ETH Library is the provider of the digitised journals. It does not own any copyrights to the journals and is not responsible for their content. The rights usually lie with the publishers or the external rights holders. Publishing images in print and online publications, as well as on social media channels or websites, is only permitted with the prior consent of the rights holders. Find out more

Download PDF: 23.10.2025

ETH-Bibliothek Zürich, E-Periodica, https://www.e-periodica.ch

Ultimate Load and Failure Mechanism of Thin Webs in Shear

Charge ultime et mécanisme de ruine des âmes minces cisaillées

Traglast und Tragmechanismus dünner schubbeanspruchter Stegbleche

MIROSLAV ŠKALOUD
Doc., CSc., Ing.
Senior Research Fellow
Czechoslovak Academy of Sciences
Institute of Theoretical and Applied Mechanics
Prague, Czechoslovakia

1. Introductory Remarks

This research project was designed as a continuation to the tests conducted jointly by K.C.Rockey and the writer during the stays of the latter in University Colleges of Swansea and Cardiff in 1966-9 /1/.

The objective was to obtain more detailed evidence regarding the stress state in the webs and flanges of steel plate girders in shear. Further it was regarded as useful to obtain some information about the behaviour of webs of higher width-to-thickness ratios than those tested in Swansea and Cardiff, since in modern metal structures deep and thin plate elements are encountered more and more frequently.

2. Test Girders and Apparatus

The general details of the test girders are given in Fig. 1, and Table 1a.

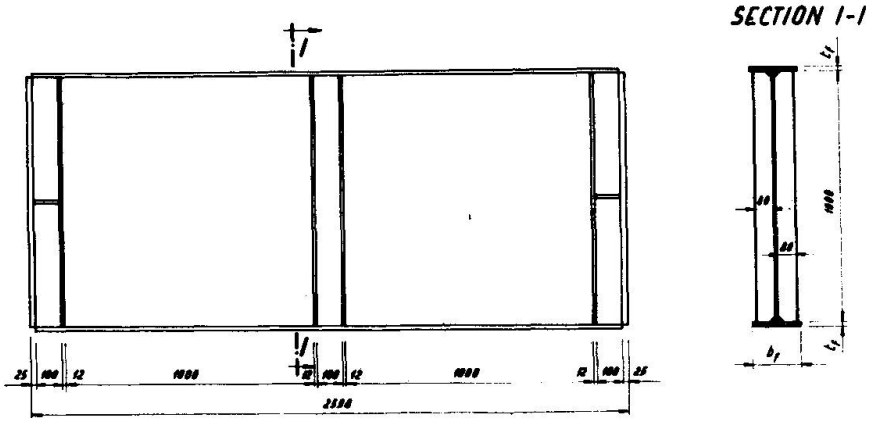

Test girder	b_f (mm)	t_f (mm)
TG1, TG1'	100	5
TG2, TG2'	200	10
TG3, TG3'	200	10
TG4, TG4'	200	20
TG5, TG5'	250	30

Fig. 1.

Table Ia.

Actual Geometrical Characteristics of the Flanges

Test Girder	b [mm]	t_f [mm]		I_f/a^3t		
		Lower flange	Upper flange	Lower flange	Upper flange	Average
TG 1	160	5,06	5,15	$0,69 \times 10^{-6}$	$0,729 \times 10^{-6}$	$0,709 \times 10^{-6}$
TG 1'	160	5,26	5,20	$0,775 \times 10^{-6}$	$0,75 \times 10^{-6}$	$0,762 \times 10^{-6}$
TG 2	200	10,08	10,00	$6,84 \times 10^{-6}$	$6,68 \times 10^{-6}$	$6,76 \times 10^{-6}$
TG 2'	200	10,12	10,17	$6,92 \times 10^{-6}$	$7,01 \times 10^{-6}$	$6,96 \times 10^{-6}$
TG 3	200	16,43	16,51	$29,5 \times 10^{-6}$	$29,9 \times 10^{-6}$	$29,7 \times 10^{-6}$
TG 3'	200	16,42	16,46	$29,5 \times 10^{-6}$	$29,6 \times 10^{-6}$	$29,55 \times 10^{-6}$
TG 4	200	20,16	20,18	$54,5 \times 10^{-6}$	$54,7 \times 10^{-6}$	$54,6 \times 10^{-6}$
TG 4'	200	20,13	20,20	$54,2 \times 10^{-6}$	$54,9 \times 10^{-6}$	$54,55 \times 10^{-6}$
TG 5	250	29,73	29,68	$218,5 \times 10^{-6}$	218×10^{-6}	$218,25 \times 10^{-6}$
TG 5'	250	29,72	29,73	$218,5 \times 10^{-6}$	$218,5 \times 10^{-6}$	$218,5 \times 10^{-6}$

The girders are of welded construction and manufactured from Czechoslovak mild steel of the series 37. The depth b and the thickness t of the web were kept constant, whereas the dimensions of the flange varied from girder to girder to obtain various flexural rigidities of the flange. The reader will notice that the width-to-thickness ratio b/t of the web was 400, and, therefore, larger than that of the above mentioned Swansea and Cardiff shear panels ($\frac{b}{t}$ = 150, 230 and 300). The aspect ratio was constant for all web panels; $\alpha = 1$.

All test girders were manufactured in two specimens; both having the same number, but one of them being differentiated by a dash.

The buckled pattern of the web was measured by means of a device consisting of nine rectangular frames on to which 81 dial gauges, graduated in units of 0,01 mm and capable of recording deflections up to 25 mm, were attached.

To evaluate the redistribution of stresses in the web in the post-buckled range, three sets of electric resistance strain gauges were mounted on to both sides of the web plate. Further batteries of strain gauges were attached to both sides of the upper and lower flanges, the objective being to study the influence of flange stiffness upon the bending and axial stresses in the flanges.

The material characteristics were determined by means of tensile tests and conducted in an Instron testing machine. The average material characteristics (yield point σ_y and ultimate stress σ_{ult}) are listed in Table Ib.

Table Ib.

Material Characteristics

Girder element	Yield stress σ_y [kp/mm²]	Ultimate stress σ_{ult} [kp/mm²]	Elongation (%)
Web plate	20,37	30,92	26,19 (δ_w)
Flange plate	28,62	42,67	34,05 (δ_f)

3. Buckled Pattern

We noted that the shape of the buckled surface was considerably affected by the flange stiffness. While in the case of a girder with flexible flanges merely one predominant buckling half wave forms, frequently accompanied with two small buckles at the web corners, the number of the buckling waves grows with the flexural rigidity of the flange. For a web fixed into very heavy flanges the buckles are more numerous so that they almost cover the whole web panel. Such a web thereby exhibits a tendency to behave as a tension field.

An analysis of the results also indicates that there is a certain tendency for the maximum web deflection w_{max} to diminish with the enlargement of flange stiffness. This is demonstrated in Fig. 2, where the ordinates w_{max} of girders TG 1,1' and TG 5, 5', are plotted. This over-all tendency appeared, however, to be disturbed by the effect of initial curvature and residual stress pattern, which resulted in the webs of not all test girders behaving correspondingly. For this reason it was not possible to define an optimum (from the point of view of web deflection) flange stiffness; as was so remarkably done by Rockey /2/ for his bolted test panels.

As the initial curvature and residual stress pattern in ordinary welded steel plate girders is likely to be similar to that of the author's test girders, it can be anticipated that for such structure elements it might frequently be difficult to base an optimum design of webs on the afore said elastic deflection approach. It is more promising to base the optimum design on the ultimate, plastic, behaviour of the girder. This concept was already used by Rockey and the author in /1/, /3/, and it is again followed below.

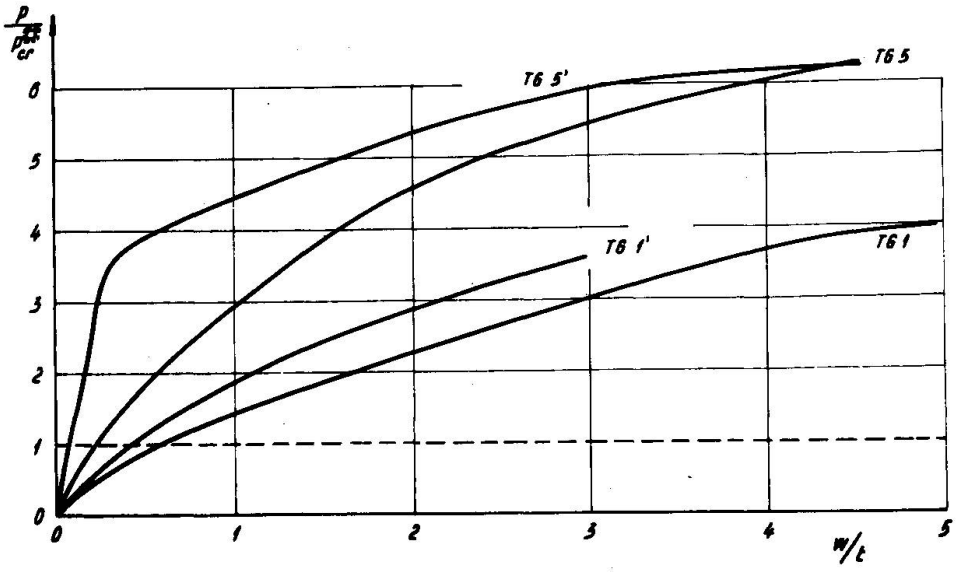

Fig. 2.

4. Stress State

4.1. Web

The strains in the web were evaluated by means of the

electric resistance strain gauges mounted on to both sides of the web of the test girders. The results relating to girders TG 1 (very flexible flanges) and TG 5 (very rigid flanges) are plotted in Fig. 3. The value ε_{cr} , corresponding to the critical load τ_{cr} of a simply supported web, and the value ε_y' , equal to σ_y/E and, therefore, relating to the yield stress σ_y of the web material, are also given in the figures for the sake of comparison. The progression of the plastification of the web is demonstrated in Fig. 4, in which the zones with plastic strain of 2 000 microstrains are plotted. Fig. 4a relates to girder TG 1, Fig. 4b to TG 3, and Fig.4 to TG 5.

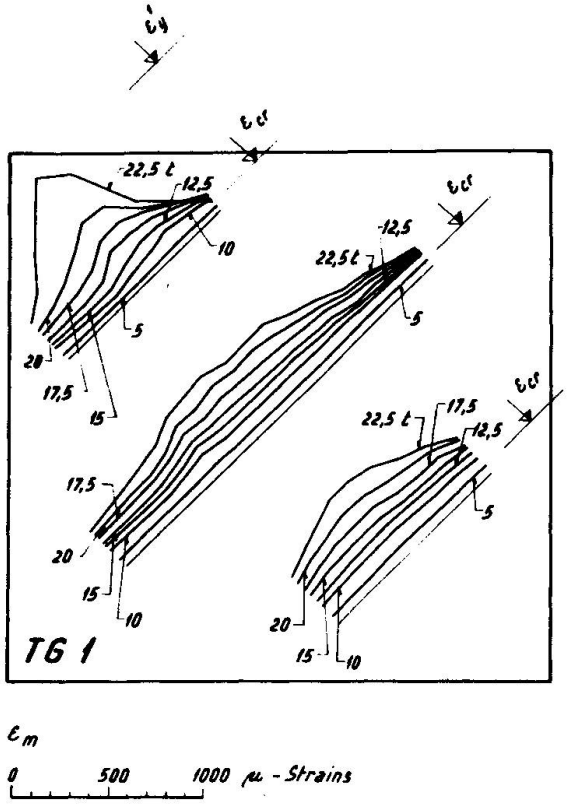

Fig. 3a.

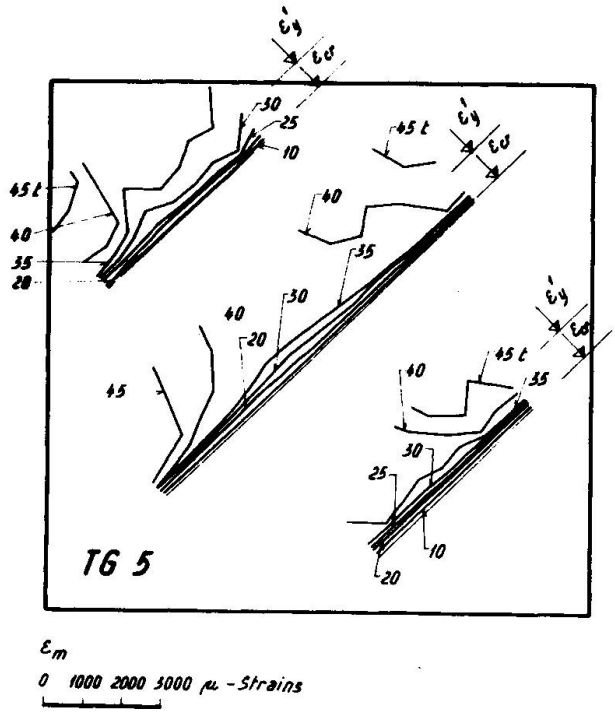

Fig. 3b.

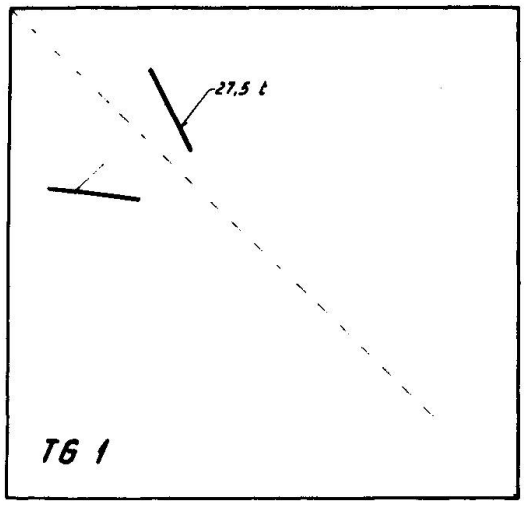

Fig. 4a.

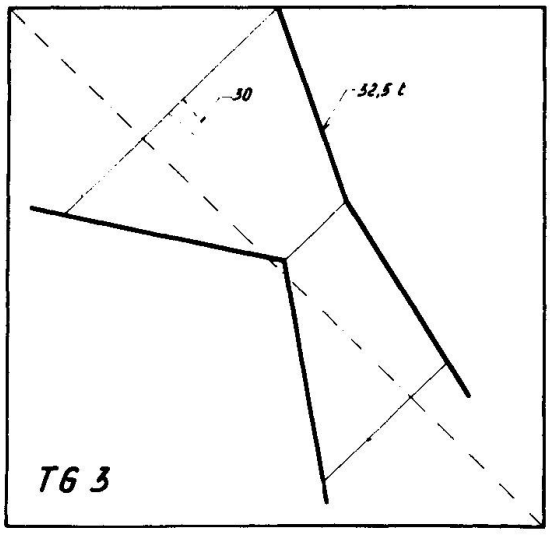

Fig. 4b.

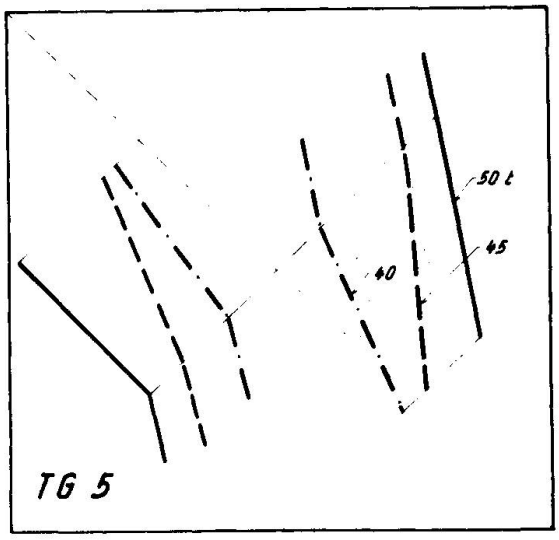

Fig. 4c.

An analysis of the results shows that a pronounced redistribution of stresses occurs in the web in the post-buckled range of its behaviour. Whereas at loads up to about the buckling load τ_{cr}, the stresses are uniformly distributed over the web ($\sigma_1 = -\sigma_2 = \tau$, σ_1 and σ_2 denoting the principal tension and compression stresses, respectively), in the postbuckled range it is the principal tension membrane stress that predominates.

Nevertheless, in the case of webs attached to flexible flanges, the stress pattern is far from a uniform tension field, whether complete or incomplete. It manifests a tendency to concentrate in a more or less narrow tension band following the tension diagonal, whereas the other web corners, situated at the ends of the compression diagonal, are idle. The more flexible are the flanges, the narrower is the tension band. As the flange stiffness increases, the width of the tension strip grows.

In the case of very heavy flanges, there is a tendency for the behaviour of the web to converge to an incomplete tension field covering the whole web. None the less, in spite of the flanges of girders TG 5 and TG 5' being very bulky, a classical incomplete tension field action has not been attained. This is a sign that the classical version of the incomplete tension field theory, established for webs fixed into completely rigid boundary elements, can very rarely be applied in the design of ordinary welded plate girders.

On the other hand, the experimental evidence shows that the tension band suggested by Basler in his very interesting contribution /4/ and assuming that its inclination equals one half of the angle of the geometrical diagonal, and that its border lines pass through the ends of the vertical stiffeners, is not fully compatible with the actual distribution of stress in a wide range of plate girder webs.

As in the preceding paragraph, where the web deformation was studied, the aforementioned analysis demonstrates the beneficial effect of flange stiffness on the post-buckled efficiency of webs in shear.

4.2. Flanges

The batteries of electric resistance strain gauges attached to both sides of each flange of the test girders enabled the bending- and axial strain occurring in the flange to be determined. The former are plotted in Fig. 5 and the latter in Fig. 6.

The bending strains demonstrate the flexure of the flange,

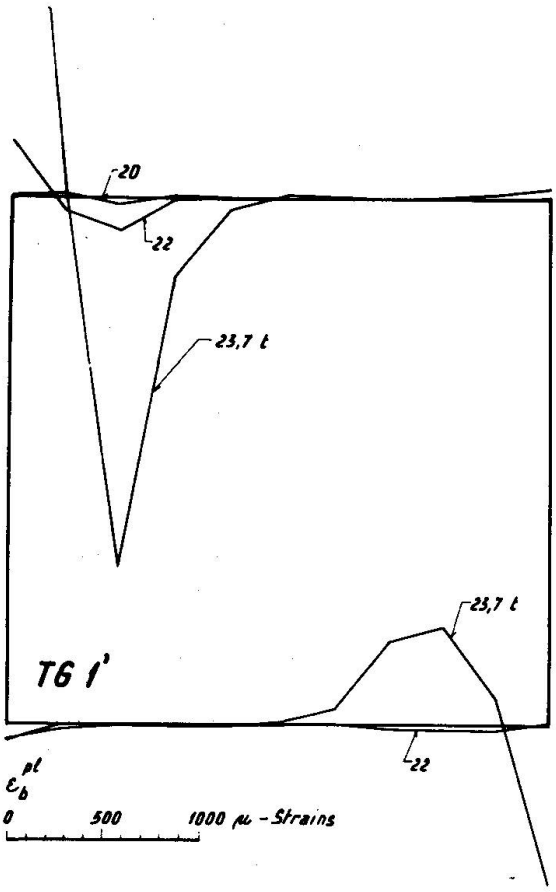

Fig. 5a.

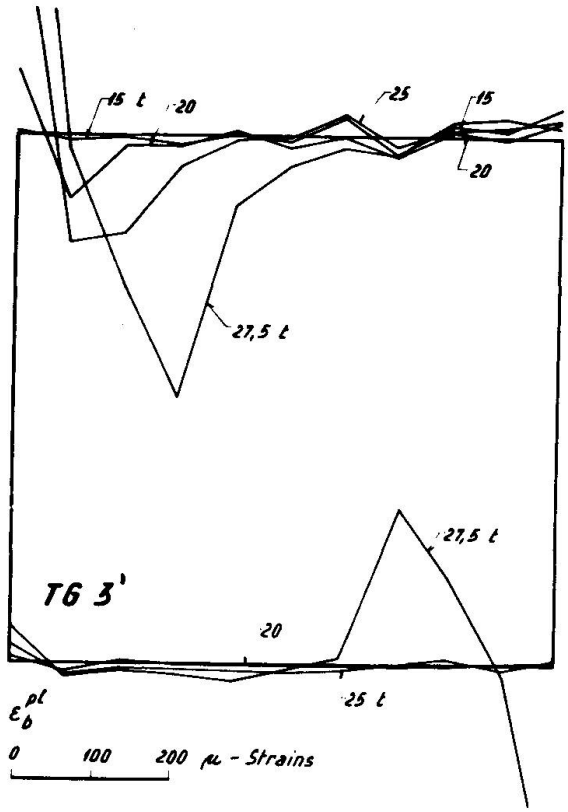

Fig. 5b.

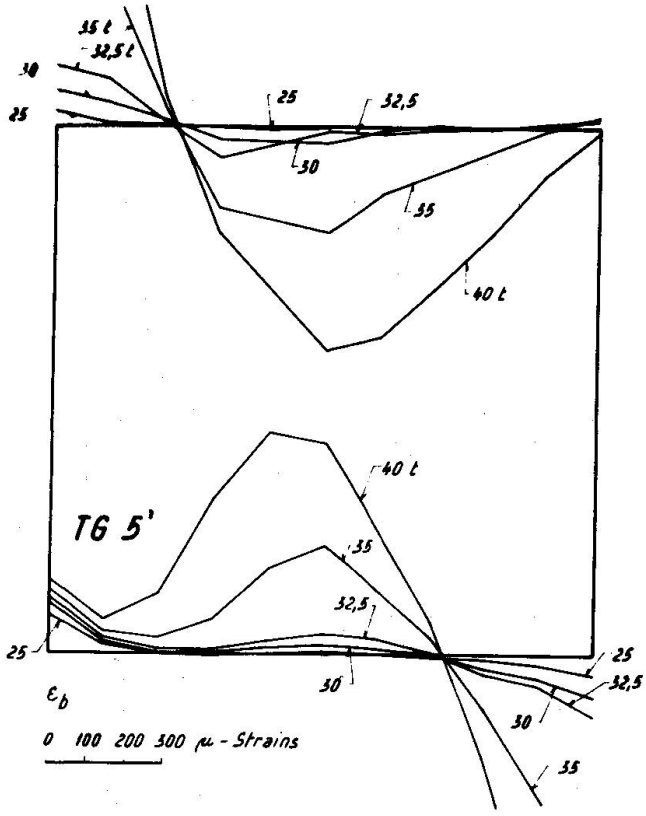

Fig. 5c.

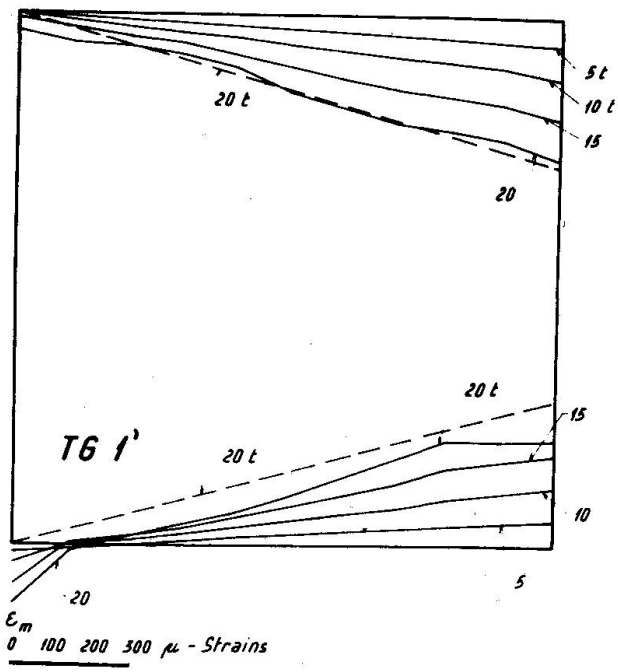

Fig. 6a.

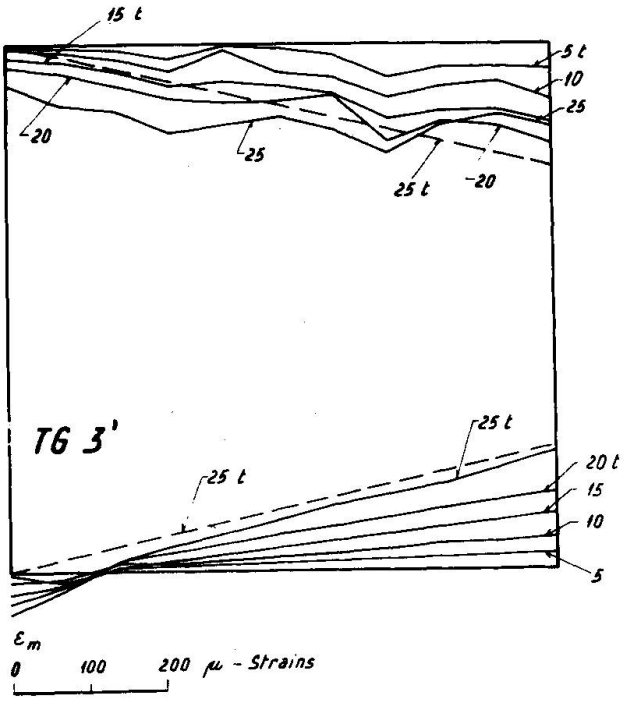

Fig. 6b.

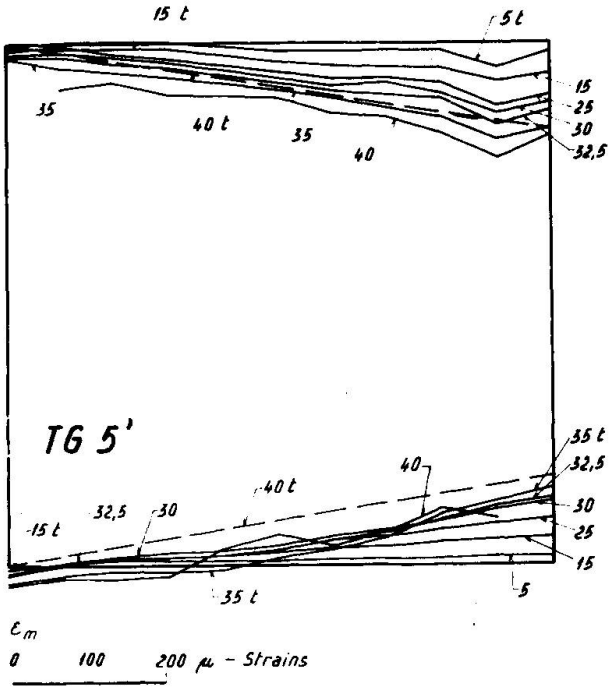

Fig. 6c.

in the middle plane of the web, under the load which is brought about by the membrane effect of the web in the post-buckled range. The bending effect is more pronounced in the compression flange than in the tension one: since compression contributes to the flange deformation and tensile stresses retard it. It can be seen that the curves have a more or less sharply defined peak, which indicates a concentration of stress in a limited portion of the flange. The more flexible is the flange, the nearer to the web corner is the stress peak. As will be shown in par. 6, plastic hinges in the flanges, playing an important part in the failure mechanism of the test girder, develop from the afore said sections of stress concentration.

The axial strains in the flanges indicate that a plate girder, with a slender web subjected to shear, is in general neither in a state of "beam action", nor in one of "truss action". Beam action would be encountered only in the case of a perfectly rigid, utterly buckling-resistant web. Then the distribution of the axial stress in the flange would be linear, as follows from the elementary formulae of "Strength od Materials" (Fig. 7). If, on the contrary, the web is extremely thin and behaves like a truss (Fig. 8), the axial force in the upper flange is uniform, and the force in the lower one is nil. The test girders exhibited the tendency to behave between the two boundary cases. It was noticed that the part played by the truss action increased with the flange stiffness. This can be explained in the light of the fact that for such girders the post-buckled strength is considerably greater (see par. 5), and, therefore, the tension field action is more developed.

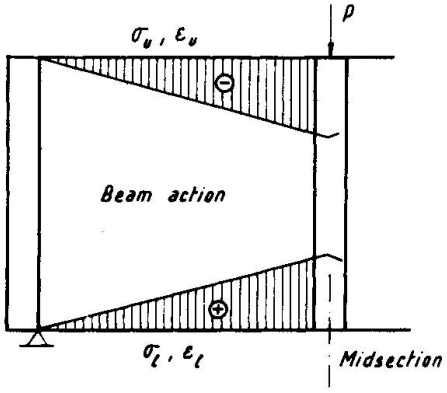

Fig. 7.

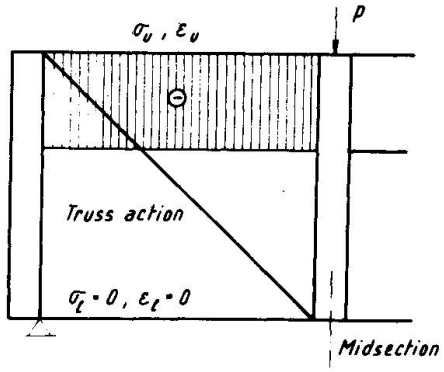

Fig. 8.

5. Ultimate Load.

The load-carrying capacities of the test girders are plotted in Fig. 9 in comparison with a) the critical loads of a simply supported web (P_{cr}) and of a web fixed into flanges and simply supported at vertical stiffeners (P_{cr}), b) the yield load in pure shear (P_y^s), c) the ultimate load determined by the theory of incomplete tension field for a web attached to perfectly rigid boundary elements ($^rP_{ult}^i$), d) the ultimate strength P_{ult}^i evaluated by Kuhn's approach to the effect of flange flexibility in tension field theories, and, e) the load-carrying capacity P_{ult}^B established by Basler's theory.

An analysis of the figure shows that the ultimate loads of the test girders very significantly grew with the flange stiffness, so indicating the benefical effect of flanges of large moment of inertia. The difference in strength between girder TG 1 and TG 5 was as great as 127 %.

Furthermore, it can be seen that the experimental load-carrying capacities of the girders with heavy flanges tend to

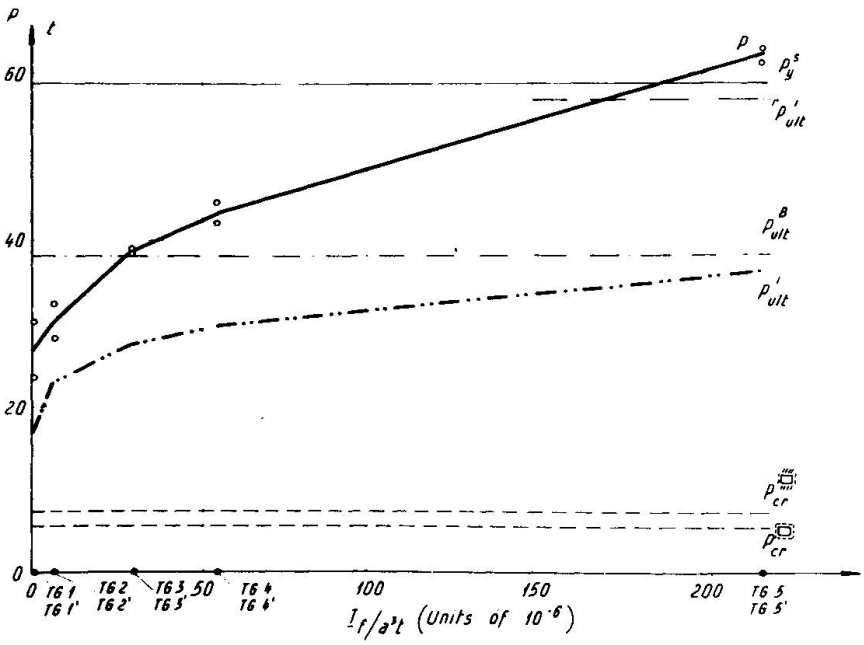

Fig. 9.

converge to the value ${}^{r}P_{ult}{}^{i}$; or, as this value is only slightly less than the yield load in pure shear, to $P_y{}^{s}$.

An inspection of the figure indicates that the ultimate loads P_{ult}^{i} , which were calculated by Kuhn's approach /5/, based on the incomplete tension field theory and with due regard to flange flexibility, were considerably lower than the experimental results and, therefore, too conservative.

On the other hand, Basler's theory appeared to give too high load-carrying capacities when flanges are flexible (the reader will recall that this theory was established for girders of this kind), but it significantly underestimates the girder strength when the flanges are heavy.

It was also of interest to find out how the beneficial effect of increased flange rigidity was affected by the width-to-thickness ratio of the web. For this reason girders with higher b/t ratio than those tested in Swansea and Cardiff were tested. The resulting P_{ult}/P_{cr}-ratios, indicating the post-buckled reserve of strength of the respective girders, are plotted in Fig. 10; compared to the same ratios for the Swansea and Cardiff experimental girders. An inspection of the figure indicates that the beneficial effect of increased flange stiffness grows with the width-to-thickness ratio of the web.

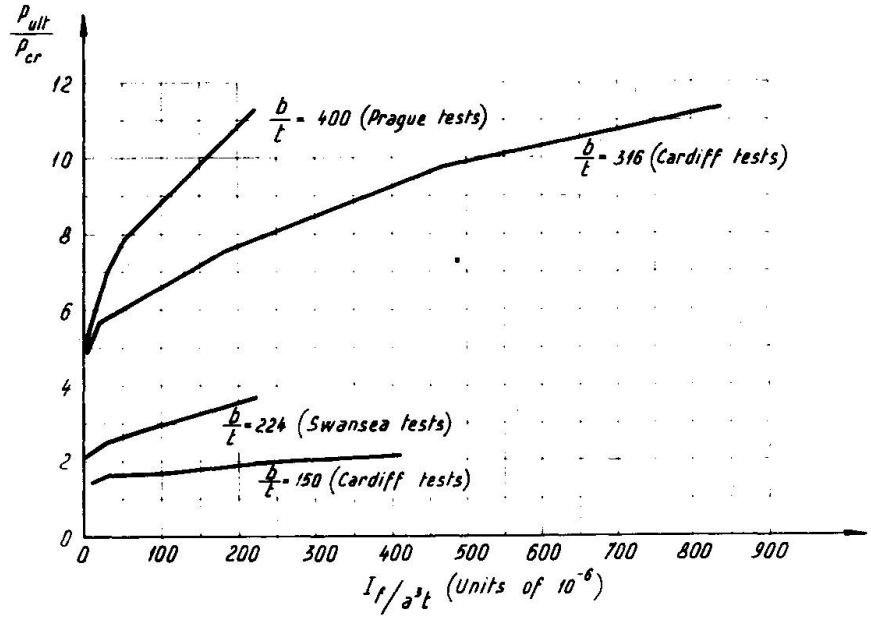

Fig. 10.

Plate girders with a web in shear and having a b/t-ratio as high as 400, as was the case for the author's test girders, can be used in ordinary steel structures (of course, subject to the fulfilment of other design requirements) provided that their flanges have a sufficient flange stiffness. Such slender webs may frequently be profitable in the case of deep large-span plate girders, where the web represents a predominant part of the weight of the whole girder.

6. Failure Mechanism

Rockey and the author discovered in Swansea and Cardiff in 1966-9 that the failure mechanism of a web panel in shear consisted of a diagonal plastic flow in the web and a system of plastic hinges in each flange.

The present experimental study has supported this finding.

In addition to it, thanks to measuring thoroughly the deformation and stress states in the web and flanges of the test girders, it was possible to obtain some evidence regarding the progression of yielding in various parts of the girder, and about its limiting state. The main conclusions will now be discussed.

6.1. Progression of Yielding and the Limiting State

The strain measurements discussed in par. 4 demonstrate the progression of yielding in a plate girder having web pannels subjected to shear. In ordinary welded steel plate girders, where initial curvature and residual stresses significantly influence their performance, the critical load P_{cr} can be exceeded, without any classical buckling phenomenon being observed (Fig.11). The load then grows on; at a value $P_{el\ max}$ the web buckling stops being elastic, and a permanent wave pattern forms.

After further increment of load, the web starts to yield at a point (or in a small zone) of one of its two surfaces; this being due to the combined action of membrane and bending stresses. The corresponding load is plotted in Fig. 11. Membrane yielding then begins over the whole web thickness, the relating load being slightly higher than that at which the aforementioned onset of surface plastification occurred. The membrane plastification propagates as the load is further increased. The force at which a plastic strain ε_{pl} = 2 000 microstrains was attained is also given in Fig. 11. When the load is further increased, a diagonal plastic band forms in the web, the web thereby losing any

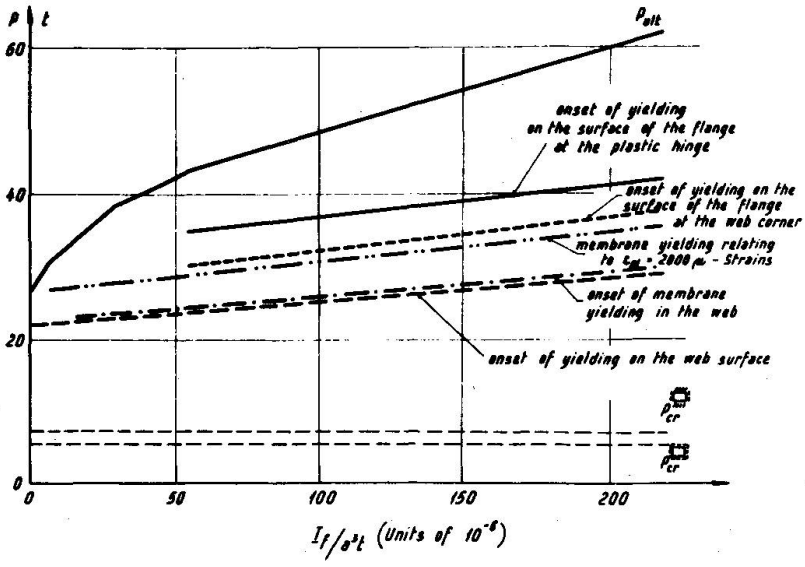

Fig. 11.

capacity to sustain any higher load; so that any additional increment in load has to be carried by the boundary frame consisting of flanges and vertical stiffeners.

The boundary framework fails when a collapse mechanism forms. Usually it is a mechanism of local failure of each flange; consisting of two plastic hinges at the frame corners (i.e. at the junctions of the flanges to the vertical stiffeners), and of another hinge between the stiffeners, situated more or less close to the web corner. The loads marking the onset of surface yielding of the flange at a) the web corners, and b) the inner plastic hinge are shown in Fig. 11. The difference between these loads on one side and the experimental collapse load curve on the other indicates a further reserve of strength provided by the stiffness of each flange.

An analysis of Fig. 11 shows that all respective loads discussed above increase with flange stiffness. thereby demonstrating the important part played by the flexural rigidity of flanges. It can also be seen there that the onset of yielding of any kind, or the sheer formation of a diagonal plastic strip in the web, does not yet mean that the limiting state of the girder has been attained. The limiting state of the girder is reached only when the aforementioned collapse mechanism forms.

6.2. Description of the Failure Mechanism

The failure mechanism of a web panel attached to flanges and vertical stiffeners, and subjected to shear, consists of a diagonal plastic band in the web and a system of plastic hinges in the boundary frame. The number of the hinges is such that a kinematic mechanism forms in the boundary framework. Usually this is a mechanism of local failure of each flange as shown in Fig. 12.

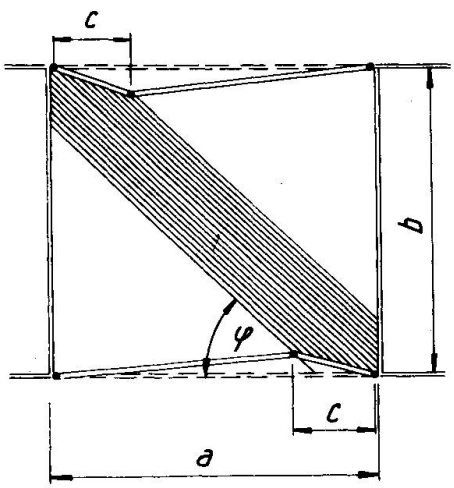

Fig. 12.

Plastic Buckled Pattern in the Web.

The contour plots of the post-failure plastic residues in web panel W_1 of girders TG 1, TG 3, and TG 5 are plotted in Fig. 13.

It will be noted there that the shape of the plastic buckled pattern is considerably affected by the flange stiffness. In the case of flexible flanges only one predominant buckling half wave forms (often accompanied by two small half waves, each of them situated near one end of the tension diagonal and on different sides of the predominant buckle). Moreover, the yielded strip is narrow. A larger number of buckling half waves, and a wider plastified area, frequently covering the whole web, occurs when the flanges are heavy.

The inclination φ of the diagonal buckles also demonstrates a tendency to grow somewhat with the moment of inertia I_f of the flange. It appears that the inclination converges to the value $\varphi_i = 45^o$, which results from the incomplete tension field theory for webs fixed into perfectly rigid boundary

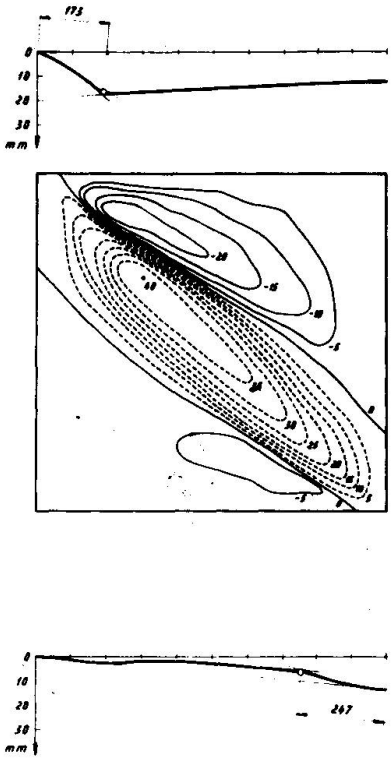

Test girder TG1 - panel W1
(post-failure plastic residue)

Fig. 13a

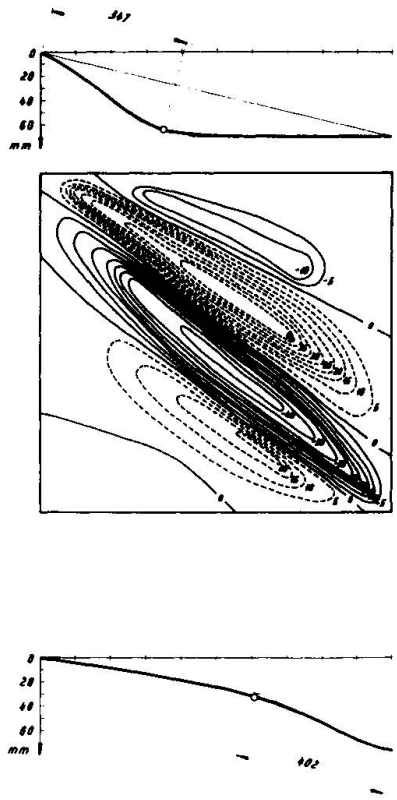

Test girder TG3 - panel W1
(post-failure plastic residue)

Fig. 13b

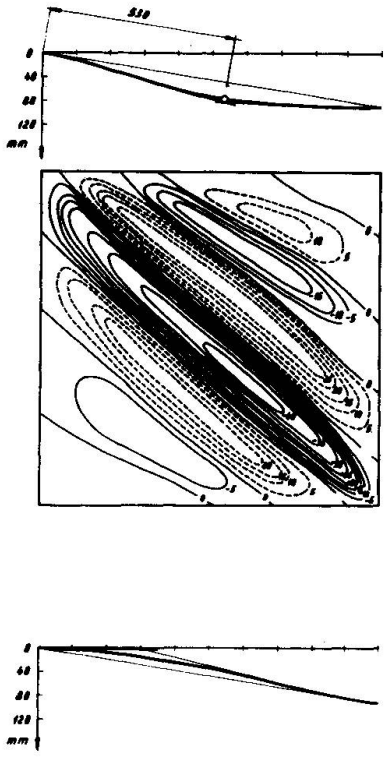

Test girder TG5 - panel W1
(post-failure plastic residue)

Fig. 13c

elements. Nevertheless, the difference between the experimental φ -values and the angle φ_d of the geometrical diagonal is small for all test girders. (Fig. 14).

Plastic Hinges in the Flanges.

A typical flange plastic hinge is shown in Fig. 15. As in the previous tests by Rockey and the author of the present paper, it was noted that the distance c of the inner plastic hinge from the web corner grew with the flange rigidity. This is illustrated in Fig. 16, where the values of c/a are plotted, in terms of I_f/a^3t, for all test girders.

Design Procedure

Using the afore said failure mechanism, Rockey and the author of the present paper established in /3/ a design procedure for webs in shear and attached to flanges of various flexural rigidities.

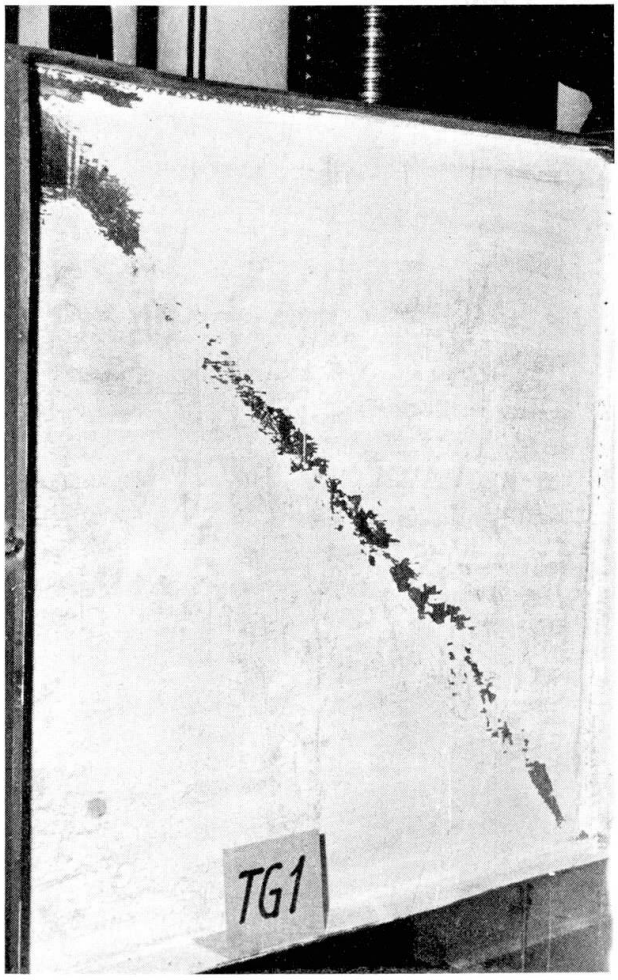

Fig. 13 d

Fig. 13 f

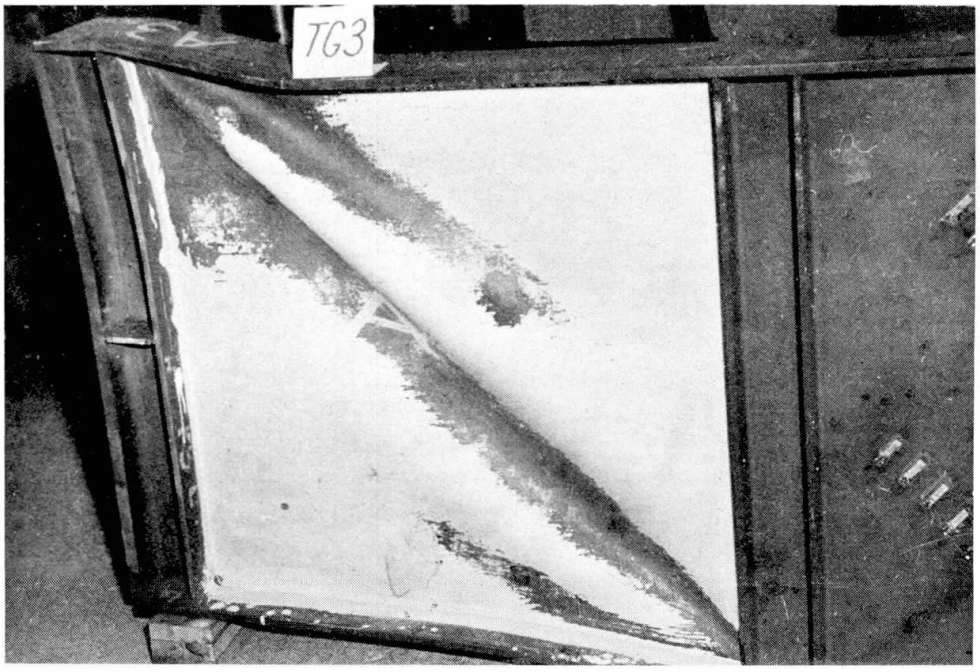

Fig. 13 e

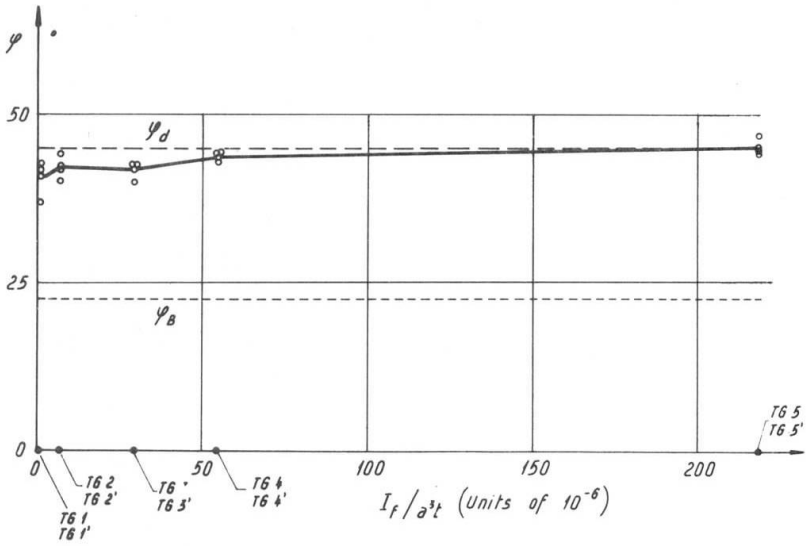

Fig. 14

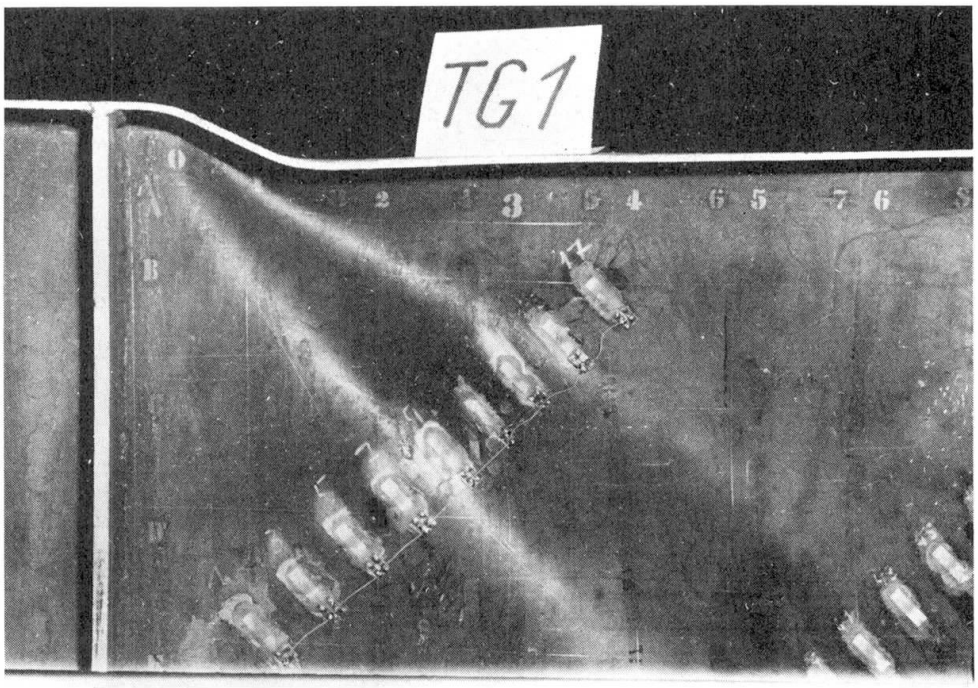

Fig. 15

This design procedure can serve as a suitable basis of an optimum design of webs in shear with regard to their post-buckled behaviour.

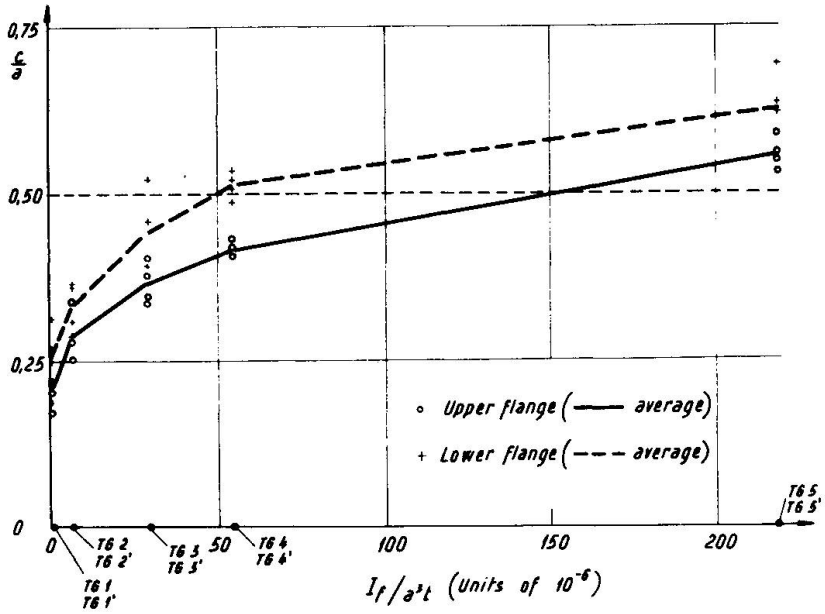

Fig. 16

References

/1/ Rockey,K.C., Škaloud,M.: Influence of Flange Stiffness upon the Load-Carrying Capacity of Webs in Shear; Report presented at the 8th Congress of IABSE, New York, September,1968

/2/ Rockey,K.C.: Plate Girder Design - Flange Stiffness and Web Plate Behaviour; Engineering, December, 1957

/3/ Rockey,K.C., Škaloud,M.: The Ultimate Load Behaviour of Plate Girders Loaded in Shear; Report of the University College Cardiff, 1970

/4/ Basler,K.: Strength of Plate Girders in Shear; Fritz Engineering Lab. Report No. 251-20, 1960

/5/ Kuhn,P., Patterson,J.O., Levin, L.R.: A Summary of Diagonal Tension - Part I - Method of Analysis; NACA - Technical Note 1952

SUMMARY

It was shown in the paper that flange stiffness very considerably affects the deformation and stress state of a web panel in shear, and the failure mechanism and ultimate load of the whole girder. A 127% increase in load-carrying capacity was achieved when the web was attached to flanges of high moment of inertia. Therefore, webs of large width-to-thickness ratios can be used provided that the flange rigidity is sufficiently high.

Leere Seite
Blank page
Page vide